NOVEL NANOCOMPOSITE INSULATION MATERIALS FOR THE ENHANCING PERFORMANCE OF POWER CABLES

Ahmed MOHAMED
Nano-Technology Research Centre
South Valley University - Egypt
ath990@hotmail.com

Youssef MOBARAK
Faculty of Engineering, Rabigh
King Abdul-Aziz University - Saudi Arabia
y_a_mubarak@hotmail.com

ABSTRACT

This paper has investigated novel nano-metric industrial materials based on Power Low Profile PLP for enhancing the electrostatic field distribution in the insulation of power cables estimated by Charge Simulation Method CSM. The electrical insulation properties of new composite materials have been enhanced by adding certain values of spherical nanoparticles of Clay and Fumed Silica in a matrix of polymer industrial materials. The size of the spherical inclusion acts as the reinforcing phase and has a major effect on the dielectric properties of composite industrial materials. Therefore, with respect to nanoparticles as the preferred reinforcing phase for the composites, the dielectric interphase has a major effect on its dielectric properties. Theoretical and experimental results have been investigated in comparison with conventional structure materials and new nanocomposite industrial materials for AC and DC power cables. Finally, this paper explained the economical cost of the new nanocomposite insulation materials related to the conventional power cables insulation materials.

INTRODUCTION

The development of nanocomposites represents a very attractive route to upgrade the old polymers without changing polymer compositions and processing. In contrast to conventional filled polymers, nanocomposites are composed of nanometer sized fillers, nanofiller which are homogeneously distributed within the polymer matrix. The conversion of bulk polymer into interfacial polymer represents the key to diversified polymer properties. As a function of the nanofiller aspect ratio it is possible to reinforce the polymer matrix and to improve the barrier resistance against gas and liquid permeation and enhance other dialectic properties. In the last few years there has been a burgeoning interest in this technology by many research groups worldwide and special sessions devoted to the subject in journals and conferences [1-3]. However, within this class of composites, there is a great deal of opportunity to tailor the properties of the resulting material to specific applications. From the viewpoint of insulating systems most of the activity has been on Clays and inorganic oxides (particularly SiO_2, Al_2O_3, ZnO and TiO_3). This paper studies the electric field distributions in various types of dielectrics of AC three core belted cable and DC cable by means of accurate determination of the magnitude of electric field within the cable. It's possible to set a limit on the voltage rating for a given insulating thickness and choice of best insulating material. For AC cable insulating electrical field calculated using charge simulation method which is a numerical method for computation of electrostatic field. Many researches in this field simulate a three core cable and improve charge simulation method to have less error [5]. The potentials of fictitious charges are taken as particular solutions of Laplace's and Poisson's equations. Physically the distributed surface charges are replaced by discrete fictitious charges. These charges are located outside the space in which the field is to be computed. The magnitude of these charges has to be calculated so that their integrated effect satisfies the boundary conditions exactly at selected number of points on the boundary. As the potential due to these charge satisfy Laplace's and Poisson's equation inside the space under consideration, the solution is unique in this space. DC cable computation of field is more complex than in AC cables [7]. The field distribution in DC cables depends on the insulation permittivity and conductivity, the geometry of the cable and the applied voltage. It is important to be able to predict the performance of insulating materials under DC stress, and to have information a best permissible stresses, and stress distribution in cable insulation.

The present study attempts to shed some light on these matters. This study is confined to steady-state conditions. The electric field is calculated by using Finite Element Method FEM for finding approximate solutions of Partial Differential Equations PDE as well as of integral equations. The solution approach is based either on eliminating the differential equation completely, or rendering the PDE into an approximating system of Ordinary Differential Equations ODE. These equations are then numerically integrated using standard techniques such as Runge-Kutta [6-8].

POWER CABLES MODEL

AC Power Cables

Recent technique uses less number of charges and gives small errors and high degrees of accuracy [6]. Assumptions which are taken into consideration will be stated as follow: All calculations used two dimension

analysis, all line conductors are considered to be cylindrical, infinitely long lines parallel with each other and parallel to a flat earth. These conductors are represented by their images, balanced three phase voltage, no free charge in space, and the permittivity is constant. In the Charge Simulation Method CSM the actual charges on the conductor surfaces are replaced by fictions line, ring or point charges. These fictions lines are placed outside the region where a field solution is desired. The magnitude of these charges should be such that the net potential is equal is to the known potential at selected number of boundary points on the conductor surface. The 8 points are shown on the right-hand core in fig.1. The values of the charges can be calculated as follows:

$$[P]_{nxn}[Q]_n=[V]_n \quad (1)$$

Where: [P] is a potential coefficient matrix, [Q] is a column vector of values of the unknown charges, [V] is the potential of the boundary points, and n is the number of the simulating charges.

The element of the potential coefficient matrix P_{ij} can be calculated as follows:

$$P_{ij}=\ln (D_i/D_{ij}) \quad (2)$$

Where: D_i is the distance of charge into origin (cable center), and D_{ij} is the distance of boundary point j to charge.

Finally, it can estimate the electrostatic field at any point (x_k, y_k) in three belted cable insulation can calculated as:

$$E_x = \sum_{i=1}^{Nt}\{(Q_j /2\pi\varepsilon)((x_k-x_i) /D_{ik})\} \quad (3)$$

$$E_y = \sum_{i=1}^{Nt}\{(Q_j /2\pi\varepsilon)((y_k-y_i) /D_{ik})\} \quad (4)$$

Total electric field at any point:

$$E =\sqrt{E_X^2 + E_Y^2} \quad (5)$$

The accuracy of simulation generated by the CSM depends on number of charges and their location, and the location of boundary point. Cross section of a three core belted cable has been illustrated in Fig. (1), which presents thickness of belted sheath t, thickness of insulation cable T, and cable conductor diameter d.

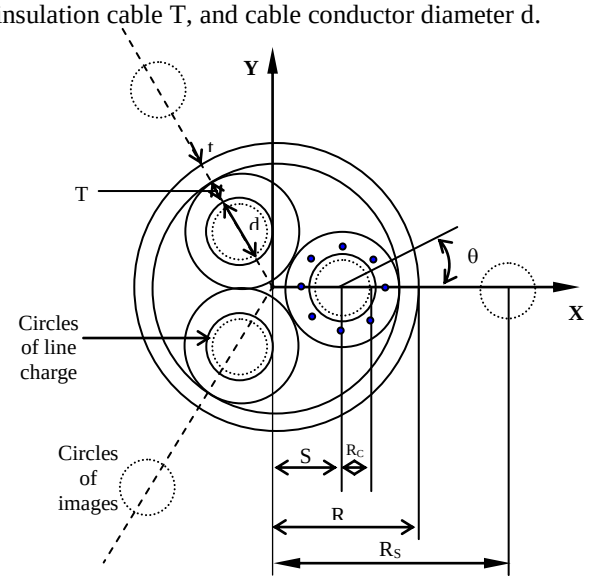

Fig.1 Cable configuration, and its coordinates axis

This type of the cable constructed normally is an insulated cable with voltage ratings below 25kV. Polymer insulated cables are almost of the sheathed type with individual cores screened, resulting in radial field distribution for each core. It's assumed that for cables, the potential and field doesn't vary with Z-direction and therefore infinite line charge are used in simulation. A total of N_C line charge are used to represent each conductor and the same number of line charges are used to represent the sheath $N_s=N_c$. The conductor charges are located symmetrically on the circumference of a circle of radius ($R_c < d/2$) whose center coincides with conductors center. The number of charge images N_s are located symmetrically on circumference of a circle of radius $R_s=R_c$ and its center lies on the line that passes through origin and conductor center, and on distance $R_s=R+T+t+d/2$ from origin, and t=0.155T.

DC Power Cables

In modeling these physical systems we must consider both perfect insulation and imperfect insulation. Figure (2) show the 30kV cable that is used in this paper. In this application, FEM applied to power cables mode. The conductor, insulation and other internal cable components are all divided into small triangular elements as shown in Fig. (3). The resulting grid (mesh) would then constitute many nodes (points) representing vertices of different triangles. The desired degree of accuracy may be obtained by adjusting the size of the grid elements. In essence, the FEM reduces the problem to that of solving a number of simultaneous algebraic equations. The steady state of the field in the first layer can be computed by insulation heating, caused by losses due to friction of the molecular polarization process in dielectric materials. A polluted insulation has a finite resistance, so that the leakage current in the insulation heats the dielectric with the following relation:

$$E = \frac{\sigma_2}{r(\sigma_2 ln\frac{r_2}{r_1}+\sigma_1 ln\frac{r_3}{r_4})} \quad (6)$$

Which r_1, r_2 and r_3 is a radius of cable core and insulation layers respectively and σ_1,σ_2 is a conductivity of insulation layers. Also, the conductivity and thermal equation used in simulation is given by:

$$J_1=\sigma_1.E_1, \text{ and } J_2=\sigma_2.E_2 \quad (7)$$

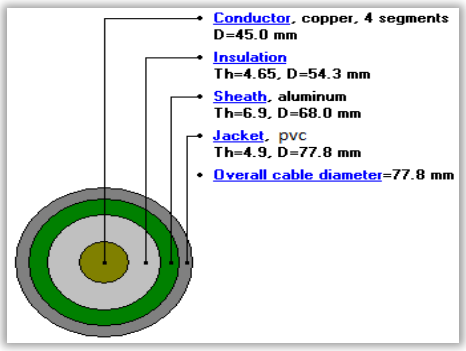

Fig. 2 DC power cable models with insulation layers

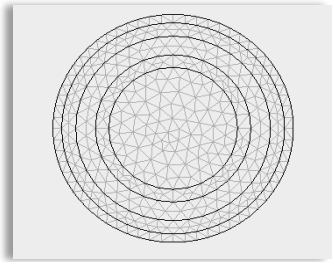

Fig 3 Meshed analysis domain model

SELECTED INDUSTRIAL MATERIALS

The presented industrial materials in this paper are PVC, and XLPE, which are used in insulating systems (AC and DC cable insulation). Although the interest here is primarily the dielectric properties of this new class of material, it is likely that many of the applications will also take advantage of attendant changes in other attributes, particularly thermal conductivity, coefficient of the thermal expansion and thermal endurance [4].

RESULTS AND DISCUSSION

Electric Field Distribution in three Core Belted Cable Insulation

Figure (4) shows the insulation materials PVC, and XLPE with different nanocomposite Clay, Glass Beads, and $BaTiO_3$. Glass Bead 15wt% composite have high electric field distribution within insulation due to its low dielectric constant, while PVC-$BaTiO_3$ 15wt % have low electric field distribution due to its high dielectric constant and other composite electric distribution graded between them.

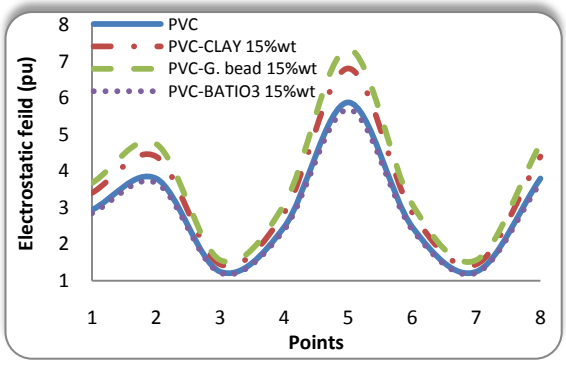

(a) PVC insulation materials

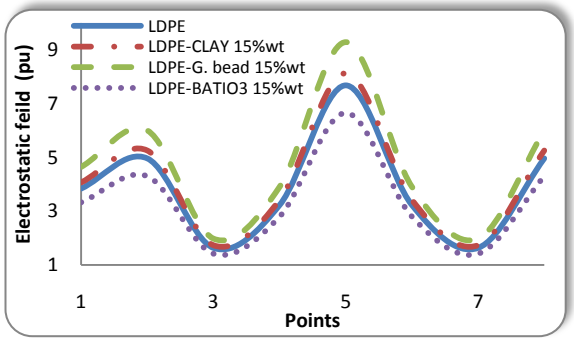

(b) LDPE insulation materials

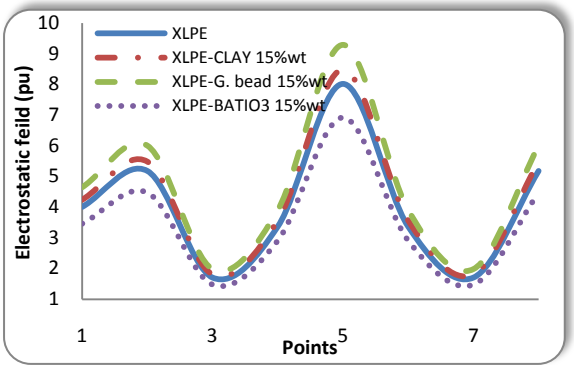

(c) XLPE insulation materials

Fig. 4 Electrostatic field distribution on insulation materials with $BaTiO_3$, Clay, and Glass Bead nanocomposites, and (15% wt, K=2.3 and at 0.3T)

Electric Field Distribution in DC Cable Insulation

Figure (5) illustrates the potential and electric field distribution through the thickness of insulation layer model. Calculation achieved using various nanocomposites insulation materials in the first layer of models (XLPE with $BaTiO_3$, Al_2O_3 and Clay nanocomposites, and (15% wt, at 0.3T). Also, XLPE-Clay 15%wt nanocomposite has high electric field distribution and low potential distribution due to its low dielectric constant. While, XLPE-AL_2O_3 have low electric field distribution and high potential distribution due to its high dielectric constant and other composite electric distribution grade between them.

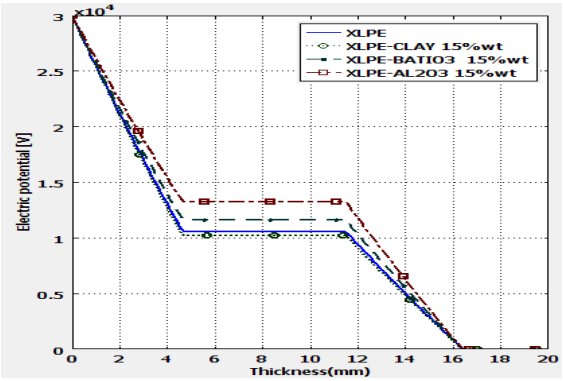

(a) Potential distribution

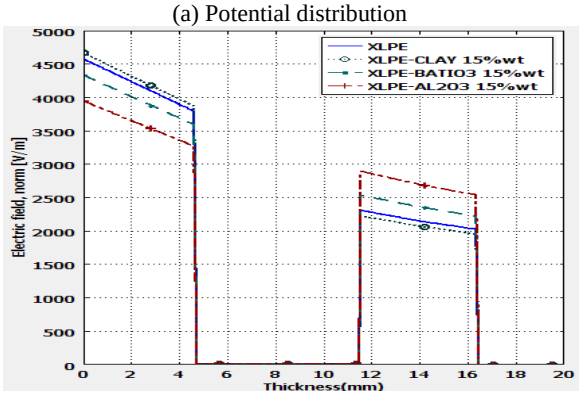

(b) Electrostatic field

Fig. 5 Potential and electric field distribution through insulation layers within different materials

Experimental Results

Figure (6) shows Hipot Tester Model ZC2674 Device, and specifications (1000VA, 20kV, AC and DC voltages, 10mA, AC and DC currents). Figure (7), illustrates the electric field distribution through the thickness of insulation layer with different nanocomposite materials. Experimental results are using PVC insulation materials with 5% Clay, and 5% Fumed Silica, as shown in Fig. (7.a). While using commercial Weak-PP-type insulation materials with 10% Clay, 10% Fumed Silica, and 10% Al_2O_3 are shown in Fig. (7.b). PVC-Clay 5%wt composite have high electric field distribution by increasing current, but PP-AL_2O_3 has high electric field distribution. Table (1) depicts the experimental electric field maximum with pure, and nanocomposite materials which are used. Dimensions of the tested samples are (3Cm dia., and 1mm thick)

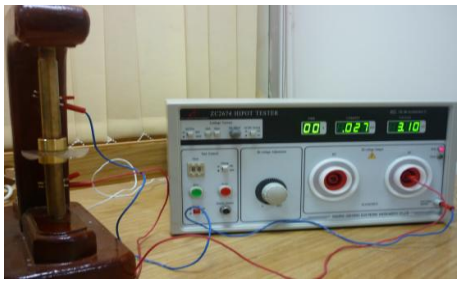

Fig. 6 Experiments results with Hipot Tester Device

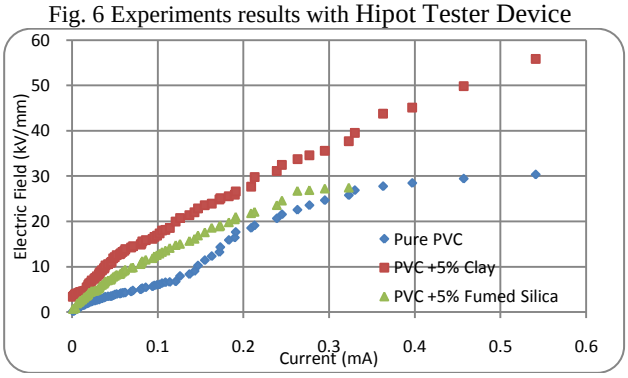

(a) PVC insulation materials

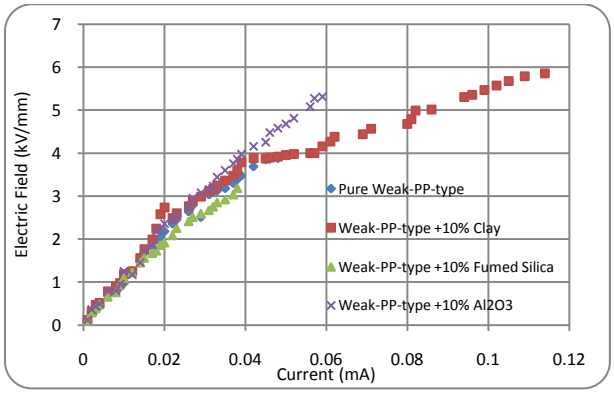

(b) PP insulation materials

Fig. 7 Electric field distribution through insulation layers within different nanocomposite materials

Table (1) Experimental Electric Field Maximum

Tested Materials	E_{max} (kV/mm)	Permittivity (ε)
Pure PVC	30.34536	6
PVC with 5% Clay	55.86538	5.06
PVC with 5% Fumed Silica	27.41848	5.61
Pure Weak-PP-type	3.940411	2.28
Weak-PP-type with 10% Clay	5.856859	1.75
Weak-PP-type with 10% Fumed Silica	3.189448	2.47
Weak-PP-type with 10% AL_2O_3	5.310458	3.05

CONCLUSION

Adding nanofillers (Clay, $BaTiO_3$, Al_2O_3) to polymer industrial materials have enhanced their electrical properties and their electrostatic field withstand strength. Adding costless nanofillers of clay has raised electric field strength of nanocomposite materials with respect to other nanofillers of (fumed silica and Al_2O_3). Thickness of insulation power cables has depend on electric field distribution withstand through nanocomposite materials which will depended on the type and percentage of added nanofillers.

ACKNOWLEDGMENTS

The present work was supported by the Science and Technology Development Fund (STDF), Egypt, Grant No: Project ID 505.

REFERENCES

[1] N. Lombardo, 2007, A Two-Way Particle Mapping for Calculation of the Effective Dielectric Response of Graded Spherical Composites, Composites Science and Technology, IEEE, Vol.67, pp.728–736.

[2] Vo H.T, Shi F.G., 2002, Towards Model-Based Engineering Of Optoelectronic Packaging Materials, Dielectric Constant Modeling, Microelectron IEEE, Vol.33, pp.409–415.

[3] Y. Murakami, et. al. 2008, DC Conduction and Electrical Breakdown of MgO/LDPE Nanocomposite, *IEEE Transactions on Dielectrics and Electrical Insulation* vol. 15, no. 1, 33-39.

[4] Ch. Chakradhar Reddy, and T. S. Ramu, 2008, Polymer Nanocomposites as Insulation for HVDC Cables – Investigations on the Thermal Breakdown, IEEE Transactions on Dielectrics and Electrical Insulation vol. 15, No. 1, 221-227.

[5] W.V. Hassenzahl, et. al., 2009, A High-Power Superconducting DC Cable, *IEEE Transactions on Applied Superconductivity*, vol. 19, no. 3, 1756-1761

[6] M. Takala, et. al., 2010, Dielectric Properties and Partial Discharge Endurance of Polypropylene-Silica Nanocomposite, *IEEE Transactions on Dielectrics and Electrical Insulation*, vol. 17, no. 4, 1259-1267.

[7] M.Q. Nguyen, et al., 2010, Silica Nanofilled Varnish Designed for Electrical Insulation of Low Voltage Inverter-fed Motors, *IEEE Transactions on Dielectrics and Electrical Insulation*, vol. 17, no. 5, 1349 – 1356.

[8] D. Pitsa, et al., 2010, Electrical Tree Growth Simulation in Nanocomposite Polymers: The role of nanoparticles and homocharges, International Conference on Solid Dielectrics, Potsdam, Germany, 1-3.